




Micro- and macroscopic aspects of prenematic fluctuations in nanoparticles-doped liquid crystalsSzymon Starzonek *Institute of Theoretical Physics and Mark Kac Center for Complex Systems Research, Jagiellonian University, Kraków, Poland*Krzysztof Górny  and Zbigniew Dendzik ^{*}*Faculty of Science and Technology, University of Silesia in Katowice, Chorzów, Poland*Dejvid Črešnar *Institute of High Pressure Physics of the Polish Academy of Sciences, Warszawa, Poland*Aleš Iglič *Laboratory of Physics, Faculty of Electrical Engineering, University of Ljubljana, Ljubljana, Slovenia*

(Received 12 July 2025; accepted 4 November 2025; published 9 December 2025)

This study combines broadband dielectric spectroscopy experiments with molecular dynamics (MD) simulations to investigate the impact of nanoparticle (NP) inclusions on pretransitional phenomena in liquid-crystal (LC) systems, specifically focusing on the relationship between nanoparticles, topological defects, and prenematic behavior. Our experimental results, using SiO₂-doped 4-Cyano-4'-pentylbiphenyl composites, demonstrate that while NP additions do not significantly alter the isotropic-nematic transition temperature (T_c), prenematic effects exhibit universal behavior, confirmed by identical critical exponents across all samples. This indicates that the fundamental character of prenematic fluctuations remains unperturbed by the nanoparticles at these concentrations. Crucially, the observed systematic decrease in dielectric permittivity with increasing NP concentration is elucidated by MD simulations. These simulations reveal that nanoparticles act as "seeds" for topological defects, specifically forcing the surrounding LC molecules into a "hedgehog" configuration. This static, defect-induced structure leads to a local antiparallel alignment and cancellation of molecular dipoles. This provides a direct microscopic mechanism for the macroscopic dielectric response, successfully bridging the micro-macro scales and highlighting the nanoparticle-induced local ordering as a key factor in modifying the dielectric properties of the composite system.

DOI: [10.1103/2dv2-4bd2](https://doi.org/10.1103/2dv2-4bd2)**I. INTRODUCTION**

Liquid-crystal (LC) systems doped with nanoparticles (NPs) are attracting growing interest due to their fundamental properties and potential for innovative applications [1–3]. Over the past two decades, an increasing number of theoretical, experimental, and applied studies have explored this topic [2–31]. The introduction of nanoparticles into a liquid-crystalline host is a promising method for modifying its physical properties, such as electrical and thermal conductivity, switching voltage, or dielectric anisotropy, without the need for new chemical synthesis [4,8,10,11,26]. Furthermore, the use of appropriate polymer substrates serving as micro-cells filled with nanoparticle-doped liquid crystals enables the creation of communication antennas and radiation sensors [24,26].

From a fundamental research perspective, a particularly interesting area is the pretransitional phenomena attending the phase transition from the isotropic phase to a mesophase [e.g., nematic (I-N), smectic (I-Sm), or chiral] [1–3,14–16,22,23,25,32]. While these effects, associated

with critical-like prenematic fluctuations, are well described for pure liquid crystals, the influence of nanoparticles on their character and universality remains incompletely understood. Extensive experimental evidence exists for nematic, smectic, and cholesteric phases doped with nanoparticles [3,5,8,14–16,22,23,32]. However, it must be emphasized that previous studies of LC + NP composites have sometimes yielded contradictory results regarding phase transition characteristics. In particular, a direct link between macroscopic measurements and the specific, microscopic arrangements of molecules around the nanoparticles has been lacking. Moreover, early theoretical models are not always corroborated by experimental findings [2–4,14–16,23]. Nanoparticles represent a promising method for modifying the physical properties of liquid crystals, such as electrical and thermal conductivity, switching voltage, and dielectric anisotropy, without the need for new chemical synthesis. They influence the local mesophase ordering in liquid crystals, while the LC matrix can facilitate their arrangement. The location of NPs or related geometrical hindrances might affect the local LC symmetry, leading to shifts in phase transition temperatures or a decrease in the switching voltage of structural transformations. The addition of NPs can significantly change the LC host system, leading to the emergence of novel meta-LC systems.

^{*}Contact author: zbigniew.dendzik@us.edu.pl

The aim of this work is to bridge this gap through an integrated approach that combines dielectric experiments with molecular dynamics simulations. We focus on verifying the universality of pretransitional phenomena in LC + NP composites and on elucidating the molecular mechanism responsible for the evolution of the dielectric constant near the I-N transition. Specifically, we seek to explain the microscopic origin of the characteristic "bending" behavior observed in the temperature dependence of the dielectric permittivity.

The dielectric method serves as a potent tool for investigating the ordering and reorientation of polar molecules, with various theories explaining such behaviors. For example, the Onsager approach is suitable for describing the isotropic phase in liquid-crystalline materials (above T_c), while the analysis of nematic phases often involves the application of theories such as Maier-Saupe, Maier-Meier, or Landau-de Gennes [1,2]. In essence, the Maier-Saupe description can be employed as an equivalent representation. It is worth noting that studies using broadband dielectric spectroscopy (BDS) have shown a significant impact of NPs on phase transitions and dynamics, with a particularly strong influence on pretransitional behavior observed at relatively low NP concentrations. This is linked to the disorder induced by NPs. Although the addition of nanoparticles generally does not significantly alter the isotropic-nematic phase transition temperature (T_c), pretransitional effects exhibit universal behavior, confirmed by identical critical exponents across all samples. This indicates that the fundamental character of pretransitional fluctuations is not perturbed by the presence of nanoparticles at these concentrations. Nanoparticles can also reduce the discontinuity of isotropic-mesophase phase transitions (ΔT^*) and mesophase-isotropic transitions (ΔT^{**}), meaning the phase transition approaches a continuous character [14–16].

For this reason, we use BDS for the precise characterization of macroscopic pretransitional anomalies and molecular dynamics [14–16,22,23,32,33]. In parallel, using molecular dynamics simulations, we visualize and analyze the local ordering of LC molecules around a nanoparticle. As we demonstrate, the combination of these two methods allows for the construction of a coherent picture in which the simulated "hedgehog" molecular configurations directly explain the experimentally observed decrease in dielectric permittivity. This approach establishes a bridge between the microscopic order and the macroscopic dielectric response of the system.

II. MATERIALS AND METHODS

A. Experiment

1. Materials

The liquid crystal used in this study was 4-Cyano-4'-pentylbiphenyl (5CB) with a purity of >99.5%, purchased from Sigma-Aldrich. Spherical silica nanoparticles (SiO_2) with an average diameter of 25 nm were obtained from US Research Nanomaterials, Inc. The nanoparticles were used as received, without any surface modification. According to the manufacturer's specifications, the nanoparticles were characterized by a low polydispersity index ($\text{PDI} < 0.3$),

which indicates a narrow size distribution and high sample homogeneity.

2. Sample preparation

Two concentrations of LC + NP composites were prepared: 0.1% and 1.0% by weight (wt/wt). Prior to dispersion, the SiO_2 nanoparticles were annealed in a vacuum to remove surface contaminants. Subsequently, a weighted amount of nanoparticles was added to the 5CB liquid crystal in its isotropic phase ($T > T_c$). The mixtures were then sonicated for several hours using an ultrasonic bath and mechanically homogenized at an elevated temperature until no visible aggregates could be detected under a polarizing optical microscope. This procedure was designed to ensure a uniform dispersion of nanoparticles within the liquid-crystal host.

3. Broadband dielectric spectroscopy

The dielectric measurements were performed using an Alpha A Dielectric Analyzer (Novocontrol, Germany). The samples were placed in a parallel-plate capacitor made of stainless steel with a diameter of 20 mm and a fixed gap of 0.2 mm. The measurements were conducted over a frequency range of $10^{-1} - 10^7$ Hz during a controlled cooling cycle from 350 to 273 K. The cooling rate was maintained at 1 K/min with a temperature stability of ± 0.02 K. An AC measurement voltage of 1 V (rms) was applied, a standard value in liquid-crystal studies, which is sufficiently low to avoid inducing field alignment in the isotropic phase. The static dielectric permittivity, ϵ_s , was determined from the real part of the complex permittivity at a frequency of 10^4 Hz.

B. Computer simulations

1. Simulation system

The molecular dynamics (MD) simulations were performed on a system consisting of a single spherical SiO_2 nanoparticle with a diameter of 6 nm (3000 atoms) immersed in a host of 10 000 5CB molecules. The system was enclosed in a cubic simulation box of $16.9 \text{ nm} \times 16.9 \text{ nm} \times 16.9 \text{ nm}$ with periodic boundary conditions applied in all three dimensions.

2. Simulation protocol

All simulations were carried out using the namd 2.14 software package. The CHARMM force field family was used to describe the interactions in the system. The 5CB molecules were modeled using the CHARMM Force Field. The SiO_2 nanoparticle was described using a dedicated, CHARMM-compatible parameter set developed for silica.

The simulations were run in the isothermal-isobaric (NPT) ensemble. The temperature was maintained using a Langevin thermostat, and the pressure was kept at 1 atm using a Nosé-Hoover Langevin piston barostat. The system was first equilibrated at 320 K for 1 ns, followed by a 3 ns production run at the target temperature of 310 K. A time step of 2 fs was used for all simulations.

C. Data analysis formalism

To quantitatively analyze the pretransitional effects observed in the isotropic phase, the following formalism was applied. The anomalous behavior of the static dielectric constant, $\varepsilon_s(T)$, in the vicinity of the I-N transition can be described by a critical-like relation [14–16,22,23]:

$$\varepsilon_s(T) = \varepsilon_s^* + a(T - T^*) + b(T - T^*)^\phi \quad \text{for } T > T_c, \quad (1)$$

where (T^*, ε_s^*) defines a point in which the continuous phase transition takes place, ϕ is a pseudocritical exponent and a, b are amplitudes. Another most useful form of Eq. (1) is its first derivative:

$$\frac{d\varepsilon_s(T)}{dT} = a + b\phi(T - T^*)^{\phi-1}. \quad (2)$$

The pretransitional anomaly can also be described from a thermodynamic perspective using the concept of Fröhlich entropy, S_F . The change in the system's entropy induced by an electric field E is proportional to the first derivative of the dielectric constant [2,32,33]:

$$S_F(T, E) = S_0(T) + \frac{1}{2} \frac{d\varepsilon_s}{dT} E^2, \quad (3)$$

where $S_0(T)$ is the entropy at zero field. The Fröhlich entropy can be regarded as the change in entropy of the system resulting from the imposition of an electric field E per unit volume.

Combining Eqs. (2) and (3) and according to the Mean-Field theory [1,2,4,30,32] one may express the Fröhlich entropy by the critical-like relation

$$\frac{\Delta S}{E^2} = \frac{a}{2} + \frac{b\phi}{2} (T - T_c)^{\phi-1}. \quad (4)$$

Let us substitute $(T - T_c)$ as z and $\frac{\Delta S}{E^2}$ by $y(z)$ and assume that $a < 0, b > 0, \phi \neq 1$, and $\phi > 0$. Then, the relation $y(z) = a/2 + b\phi/2z^{\phi-1}$ can be examined in terms of its dependence on parameter ϕ .

This formulation is equivalent to Eq. (2) and provides a thermodynamic basis for analyzing the pretransitional ordering effects observed in the dielectric response.

To analyze the structural and dynamic properties of the simulated system, several key quantities were calculated from the molecular dynamics trajectories.

The global degree of nematic order is quantified by the scalar order parameter, s , defined as the ensemble average of the second Legendre polynomial, P_2 [1,2]:

$$s = \frac{1}{2} (3\langle \cos^2\theta \rangle - 1) \equiv \langle P_2(\cos^2\theta) \rangle, \quad (5)$$

where θ is the angle between the long axis of a liquid-crystal molecule and the director, which represents the average orientation axis of the system.

To characterize the local ordering of molecules with respect to the nanoparticle, the radial order parameter, s_r , was calculated. It is defined similarly to the global order parameter, but the angle θ_r is the angle between the long molecular axis and the radial vector originating from the center of the nanoparticle. The average is performed for all molecules within a thin spherical shell at a distance r .

The rotational dynamics of the molecules were investigated by calculating the time autocorrelation function of the

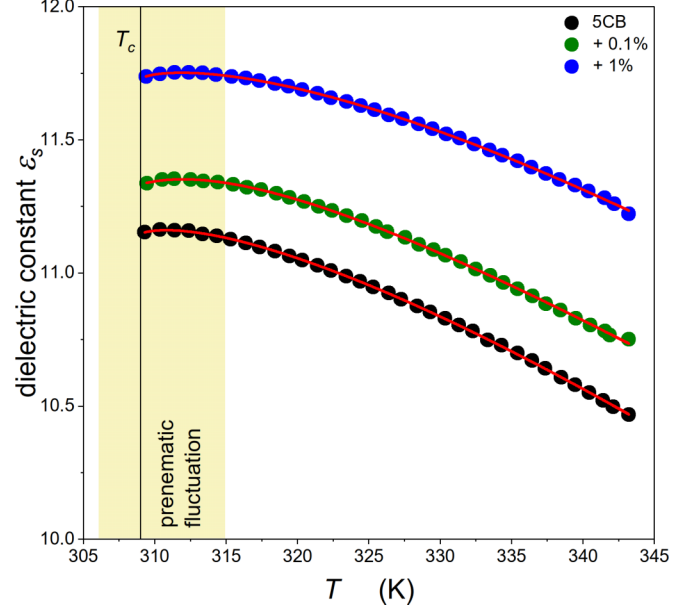


FIG. 1. Temperature evolution of dielectric constant (ε_s) in the isotropic phase of pure 5CB liquid crystal and nanoparticles-doped mixtures. In the vicinity of the isotropic-nematic phase transition temperature T_c a strong pretransitional anomaly occurs.

system's total dipole moment, $M(t)$ [2,7,17–20,29]:

$$\Phi_{\vec{M}} = \frac{\langle \vec{M}(0)\vec{M}(t) \rangle}{\langle \vec{M}(0)\vec{M}(0) \rangle}, \quad \vec{M} = \sum_{i=1}^N \vec{\mu}_i, \quad (6)$$

where $M(t)$ is the vector sum of all molecular dipole moments at time t .

III. RESULTS AND DISCUSSION

A. Dielectric response and pretransitional anomalies

Figure 1 presents the temperature dependence of the static dielectric constant, ε_s , for pure 5CB and for its composites with 0.1% and 1% NP concentrations. In all samples, a distinct pretransitional anomaly, characterized by a "bending" of the $\varepsilon_s(T)$ curve, is observed in the vicinity of the I-N phase transition temperature, T_c . This well-known effect is attributed to the formation of prenematic fluctuations; within these dynamic domains, the antiparallel arrangement of permanent dipole moments leads to their partial cancellation and a consequent reduction in the measured dielectric constant. A key observation from our data is that while the addition of nanoparticles does not significantly alter the transition temperature itself, it leads to a systematic decrease in the overall magnitude of the dielectric constant across the entire isotropic phase.

To analyze this pretransitional behavior more quantitatively, the first derivative of the dielectric constant with respect to temperature, $\partial\varepsilon_s/\partial(T)$, is plotted in Fig. 2. This derivative is directly proportional to the change in the system's entropy induced by an electric field, known as the Fröhlich entropy ($\Delta S/E^2$), which is plotted on the right axis of Fig. 2. The crossover of the derivative from positive to negative values upon heating through T_c corresponds to a change from a more

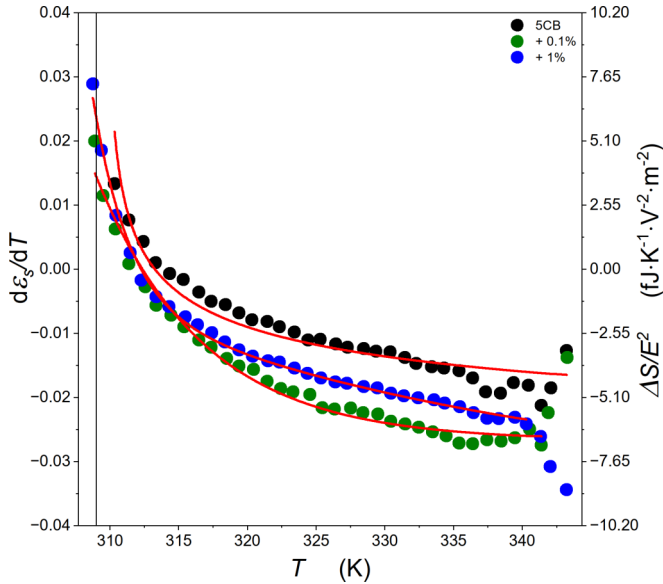


FIG. 2. The first derivative of dielectric constant $\partial\epsilon_s/\partial T$ and Fröhlich entropy $\Delta S/E^2$ taken from Eq. (4) for pure and nanoparticles-doped 5CB. The Negative value of $\Delta S/E^2 < 0$ is related to a disordered phase (isotropic), whereas positive $\Delta S/E^2 > 0$ is related to an ordered one (prenematic).

ordered state ($\Delta S/E^2 > 0$) in the prenematic region to a disordered state ($\Delta S/E^2 < 0$) in the isotropic phase. This provides a thermodynamic interpretation of the pretransitional ordering. The increased scatter of the data points at temperatures above 335 K, far from the critical region, can be attributed to a lower signal-to-noise ratio. To further characterize the nature of the anomaly, the data in the pretransitional region ($T > T_c$) were fitted using the critical-like relation described by Eqs. (2) and (4). The dashed red lines in Fig. 2 represent the best fits to the experimental data. A crucial outcome of this analysis is that the determined critical exponents, which describe the nature of the singularity, are found to be identical for both the pure and the NP-doped systems within the experimental error. This result provides strong evidence for the universality of the critical phenomena governing the I-N transition, indicating that the fundamental character of the prenematic fluctuations is not perturbed by the presence of the nanoparticles at these concentrations.

However, while the character of the pretransitional effects remains universal, the systematic decrease in the magnitude of ϵ_s upon NP doping requires a microscopic explanation. To elucidate the molecular-level origin of this behavior, we subsequently turned to molecular dynamics simulations.

B. Microscopic origin of the dielectric behavior

To elucidate the molecular-level mechanism behind the observed decrease in dielectric permittivity upon NP doping, we performed MD simulations. The simulation cell, containing a single SiO_2 nanoparticle within a 5CB host, is visualized in Fig. 3. The results reveal the formation of distinct, highly ordered layers of LC molecules around the nanoparticle. Specifically, a layer of molecules arranged radially with respect to the nanoparticle's surface forms a structure referred

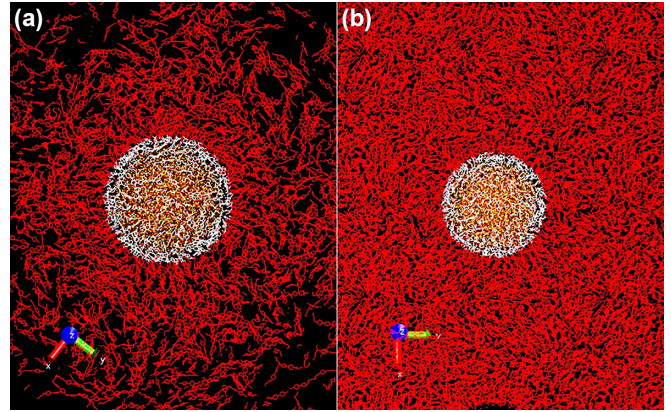


FIG. 3. The simulation cell at $T = 310$ K, nanoparticle diameter $2r = 6$ nm. Molecules in the planar layer are marked in white. In part (a), a clearly visible ordered layer forms a *hedgehog*-like structure. Part (b) takes into account periodic boundary conditions.

to as a *hedgehog*. This local ordering was quantified by calculating the radial order parameter, s_r , as a function of distance from the center of the nanoparticle, shown in Fig. 4. The plot exhibits a sharp negative dip, reaching $s_r \approx -0.38$, which corresponds to a thin planar layer of molecules directly at the nanoparticle surface. Immediately following this layer, a prominent positive peak with $s_r \approx 0.25$ is observed, which is the quantitative signature of the radially aligned *hedgehog* structure. Beyond this ordered region ($r > 40$ Å), the order parameter decays to zero, indicating the bulk isotropic phase. These simulations provide clear evidence of a static, NP-induced local order that persists within the globally isotropic phase.

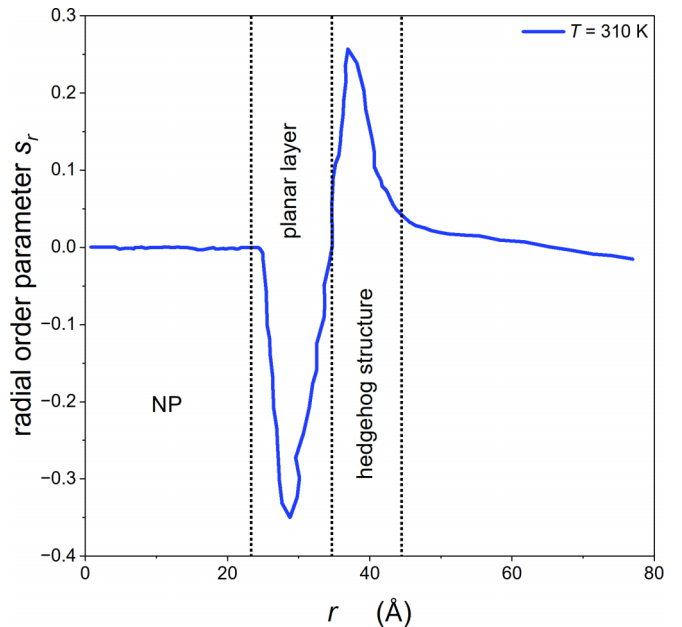


FIG. 4. Radial order parameter s_r as a function of distance from the center of the nanoparticle in a simulated system based on 5CB at a temperature $T = 310$ K.

It should also be noted that the radial symmetry of the hedgehog configuration, imposed by a spherical nanoparticle, can lead to more complex states than simple local uniaxial ordering. In the thin layer surrounding the nanoparticle, where surface curvature plays a significant role, the cylindrical symmetry around the local director is broken. This may lead to the emergence of local biaxial order, even while the bulk liquid crystal remains in the isotropic phase. This issue presents an interesting direction for future, more detailed simulation studies [34,35].

C. Molecular arrangement and dielectric permittivity

The simulation results provide a direct microscopic explanation for the experimentally observed decrease in the dielectric constant. The 5CB molecule possesses a strong permanent dipole moment aligned along its long axis. The hedgehog structure, characterized by the radial alignment of these molecules around the nanoparticle, therefore imposes an antiparallel arrangement of their dipole moments when considered over the entire nanoparticle surface.

This antiparallel configuration leads to a local cancellation of the dipolar contributions to the permittivity in the immediate vicinity of each nanoparticle. Consequently, each nanoparticle and its ordered shell effectively create a domain with a significantly reduced local dielectric constant. Since the macroscopic measurement averages the dielectric response over the entire sample volume, the presence of these low-permittivity domains results in a lower overall value of the measured $\epsilon_s(T)$. This effect becomes more pronounced with increasing nanoparticle concentration, which is fully consistent with the experimental data presented in Fig. 1.

It is important to note that the nanoparticle, with its induced static shell of prenematic order, acts as a seed that locally mimics the antiparallel dipolar arrangement found in dynamic critical fluctuations. These two phenomena—one static and extrinsic, the other dynamic and intrinsic—coexist, and both contribute to the overall dielectric response of the system.

D. Nanoparticle-induced disorder

The influence of nanoparticles on the liquid-crystalline host must be precisely classified within the theoretical framework of disorder. Two fundamental types of disorder are distinguished: annealed disorder, where the disorder-inducing elements (e.g., impurities) are mobile and reach thermodynamic equilibrium with the host medium, and quenched disorder, where the disorder is static on the time scale of the system's primary dynamic degrees of freedom. In our system, although the nanoparticles undergo Brownian motion within the 5CB matrix, their diffusion occurs on a much slower time scale (microseconds to milliseconds) compared to the ultrafast reorientational dynamics of the liquid-crystal molecules (picoseconds to nanoseconds) [12,27,36,37]. From the perspective of the prenematic fluctuations, the nanoparticles therefore constitute a static, "frozen" energy landscape. Consequently, the disorder introduced by the SiO₂ nanoparticles in the 5CB liquid crystal is unequivocally of the quenched disorder type.

The Imry-Ma theorem describes how even slight random disorder can drastically change the behavior of systems

undergoing continuous symmetry breaking. It predicts that instead of a perfectly uniform ordered phase, the system will break down into domains of short-range order, where the local ordering aligns with the fluctuating random field [14–16,24–31,38,39]. This competition between the system's tendency to order uniformly and the local influence of disorder leads to a characteristic domain length. The nanoparticles introduce a random field-type disorder into the system, as each particle, through surface anchoring interactions, imposes a local orientational preference at a random position within the sample. Key to understanding why this disorder does not significantly alter the phase transition temperature, T_c , at the studied concentrations is a quantitative comparison of the system's characteristic length scales. We have calculated the average interparticle distance (d_{NP}) for both concentrations, using the densities of 5CB ($\rho_{LC} \approx 1.01 \text{ g/cm}^3$) and amorphous SiO₂ ($\rho_{NP} \approx 2.0 \text{ g/cm}^3$). For the 0.1% wt/wt concentration, we find $d_{NP} \approx 253 \text{ nm}$, and for 1.0% wt/wt, $d_{NP} \approx 117 \text{ nm}$ [14–16,22,23,25]. These values must be compared with the nanoparticle diameter ($D_{NP} = 25 \text{ nm}$) and the temperature-dependent nematic correlation length, $\xi(T)$. For 5CB, $\xi(T)$ grows upon approach to T_c but only reaches values on the order of tens of nanometers in the immediate vicinity of the transition ($< 1 \text{ K}$) [40–44].

Our quantitative analysis thus demonstrates that for both concentrations, $d_{NP} \gg D_{NP}$, and d_{NP} is significantly larger than the size of the "prenematic cloud" [$D_{NP} + 2\xi(T)$] surrounding each particle. This confirms that our experiments were conducted in the dilute, noninteracting disorder regime. In this regime, each nanoparticle acts as an isolated perturbation and does not disrupt the collective, bulk nature of the phase transition, which explains the observed stability of T_c . At the same time, theory predicts that quenched random disorder can "smear" first-order phase transitions, driving them toward a more continuous character. The reduction in the transition's discontinuity, as suggested by our results and observed in similar systems, is therefore fully consistent with this theoretical framework [14–16,22,23,25,45–47]. According to the Imry-Ma theorem, even an infinitely weak random field-type disturbance, in the presence of continuous symmetry breaking, creates a domain pattern with short-range order. The resulting arrangement shows short-range order, described by a single characteristic domain length. In samples with NPs, the induced disorder is correlated, making it much weaker, but still strong enough to cause some glasslike features [14–16,22,23,25].

E. Nematic order parameter

For thermotropic liquid crystals characterized by a phase transition from the isotropic phase to the nematic phase, the phase transition temperature is simultaneously the critical temperature $T_{IM} \equiv T_c$. From a mesoscopic point of view, the orientational order is described by a tensor order parameter \underline{Q} . In the case of uniaxial alignment, it takes the form [1–3,5,9,14,16,21,23]

$$\underline{Q} = s(\bar{n} \otimes \bar{n} - \underline{I}/3), \quad (7)$$

where \bar{n} is identified as the local uniaxial order vector (director), s is a uniaxial order parameter measuring the size

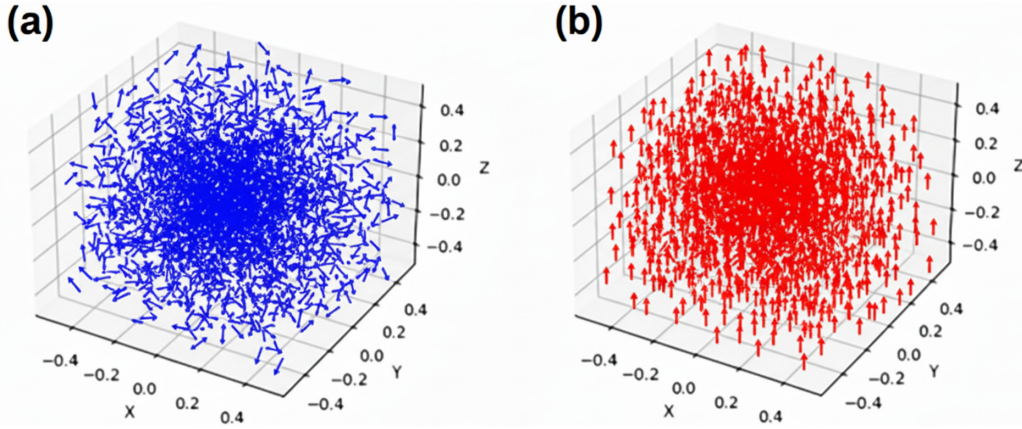


FIG. 5. Macroscopic view on dipole moments orientation in (a) isotropic ($T > T_c$) and (b) nematic ($T < T_c$) phases. The order parameter for isotropic liquid $s = 0$ and for nematic can be expressed by Eq. (5).

of fluctuations around the direction of alignment, and \underline{I} is the unit tensor. In the simplest case, such as the nematic phase, the order parameter s is defined as follows Eq. (5) [1,3,14,16–21].

Figure 5 presents the orientation of dipole moments in the isotropic (a) and nematic (b) phases. Note, that for isotropic liquid the global ordering equals to zero ($s = 0$), whereas in nematics is expressed by Eq. (5). Moreover, this equation assumes uniform values of the angle θ for all particles in the system. It is also worth emphasizing that the order parameter s is equivalent to the Legendre polynomial of the second degree $\langle P_2 \rangle$. The nematic phase differs from the isotropic phase by the value of the order parameter s , which ranges between 0.3 and 0.5 for the former, while it is zero for the isotropic liquid [2,7].

To determine the value of the macroscopic order parameter s , from dielectric data without direct measurements of the dielectric anisotropy, the Haller approximation can be used. This empirical equation relates the order parameter to temperature:

$$s = \frac{\Delta \varepsilon_s}{\varepsilon_\infty - \varepsilon_0} = s_{\text{iso}} + \left[1 - \frac{T}{T_c^*} \right]^{\beta_c}, \quad (8)$$

where s_{iso} is the order parameter of the isotropic phase (assumed to be zero), T_c^* is a hypothetical continuous transition temperature slightly above the actual clearing point T_c , and β_c is a pseudocritical exponent. While this equation was formulated for homogeneous systems, it serves as a useful approximation to compare the ordering trends in the pure and nanoparticle-doped systems.

Figure 6 shows the temperature dependence of the order parameter s , calculated using Eq. (8) for the experimental data. The results for the pure 5CB are compared with literature data from optical measurements and computer simulations. The most crucial aspect illustrated in the graph is the increase in the system's order with the rise in nanoparticle concentration, particularly for the 0.1% admixture. This suggests the presence of a strong ordering interaction between the nanoparticles and the liquid-crystal molecules, which is consistent with the formation of ordered hedgehog structures observed in the simulations.

It should be emphasized that the determination of the macroscopic order parameter, s , in such a heterogeneous composite system is a nontrivial task. Methods based on dielectric anisotropy measurements, such as the Haller approximation, are strictly defined for homogeneous, uniaxial systems. In our case, the measured anisotropy is a resultant response originating from both the bulk liquid crystal and the structurally and dielectrically complex regions surrounding the nanoparticles.

DATA AVAILABILITY

The data that support the findings of this article are not publicly available. The data are available from the authors upon reasonable request.

APPENDIX A: THEORETICAL FRAMEWORK

1. Dielectric properties of anisotropic media

The electric permittivity is described as a second-rank tensor for anisotropic media such as liquid crystals, where the electric displacement field D is related to the electric field E by $D = \varepsilon \varepsilon_0 E$. For uniaxial phases like nematics, with the director \vec{n} aligned along the z axis, this tensor has two principal components: ε_{\parallel} (parallel to \vec{n}) and ε_{\perp} (perpendicular to \vec{n}). The dielectric anisotropy is then defined as $\Delta \varepsilon_s = \varepsilon_{\parallel} - \varepsilon_{\perp}$ [1,2,14,15].

According to the Maier-Meier approach, for molecules with a permanent dipole moment μ at an angle θ with the long molecular axis, the components of the squared dipole moment are related to the scalar order parameter s by [1,2,14]

$$\langle \mu_{\parallel}^2 \rangle = \frac{1}{3} \mu^2 [1 - (3 \cos^2 \theta - 1)s], \quad (A1a)$$

$$\langle \mu_{\perp}^2 \rangle = \frac{1}{3} \mu^2 [1 + \frac{1}{2}(3 \cos^2 \theta - 1)s]. \quad (A1b)$$

2. Model of nanoparticle-liquid-crystal interactions

To consider the influence of nanoparticles on pretransitional effects, we use a simple model of a binary system. We assume the nanoparticles are homogeneously dispersed in the liquid-crystal medium and that the coupling is sufficiently

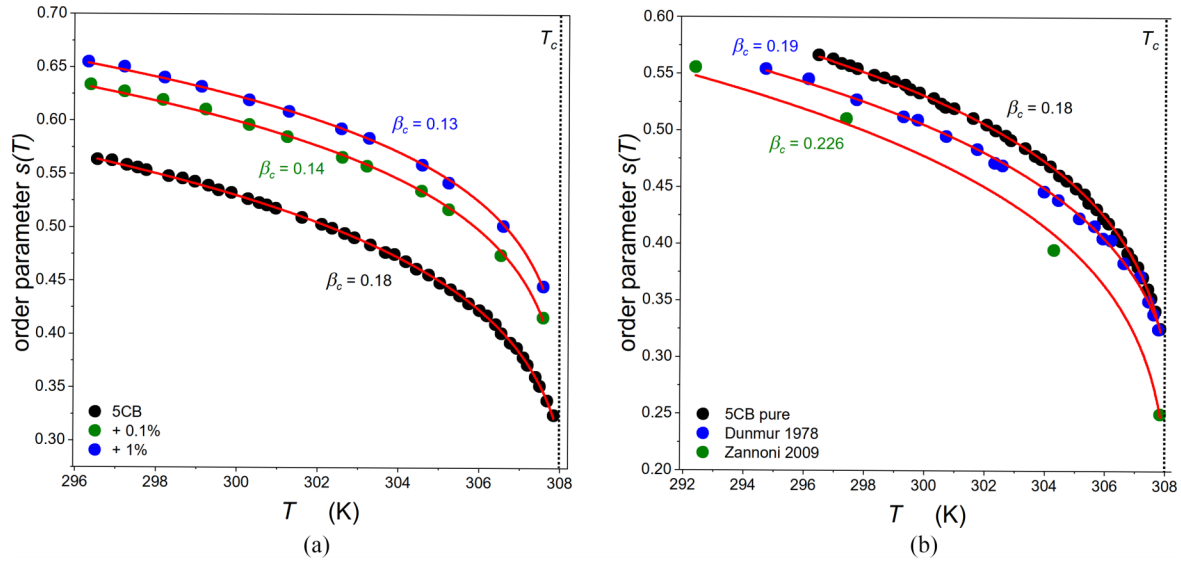


FIG. 6. (a) Order parameter $s(T)$ calculated from Eq. (8) for experimental dielectric measurements in nematic phase for various systems based on 5CB liquid crystal. (b) The comparison of the order parameter $s(T)$ calculated from dielectric data, optical measurements [16–18], and computer simulations [2,7,19–22] for nematic 5CB. Red line denotes Haller function [Eq. (8)] fit with given pseudocritical exponents.

weak to not introduce topological defects in this simplified model. The nanoparticles act as seeds for prenematic (weakly ordered) clusters. The free-energy density of such a binary system can be described as [9,16–18,23–25]

$$f = (1 - p_{cl})f_{LC} + p_{cl}f_{cl} + p_{cl}(1 - p_{cl})f_{int}, \quad (A2)$$

where $f_{LC} = A_0(T - T^*)s^2 - Bs^3 + Cs^4$, $f_{cl} = a_0(p^* - p_{cl})s_{cl}^2 - bs_{cl}^3 + cs_{cl}^4$, and $f_{int} = Ws_{cl}s$. Here, s and s_{cl} define the nematic and prenematic order, respectively. The parameters A_0 , B , C , and T^* for bulk 5CB are well established in the literature, and in our model, they are treated as constants, consistent with experimental data. The key element is the interaction term, f_{int} , where the coupling constant, W , serves as the sole fitting parameter. Physically, W reflects the strength

of the anchoring interaction of 5CB molecules on the SiO_2 surface. Anchoring energy values for similar systems are on the order of 10^{-4} J/m². Our fit yields a value for W that is in full agreement with these literature estimates, which lends the model a physical credibility that extends beyond a purely phenomenological description [48–51].

In the situation where $s_{cl} > 0$, the liquid-crystal component experiences an external field coupling term $f_{int} = -ws$. This can potentially cause a shift in the transition temperature T_c towards higher values. In real systems, however, f_{int} is very strongly spatially dependent. It does not have a globally uniform effect of the liquid-crystal component. Therefore, in a diluted regime we expect that the phase transition behavior, specifically the value of T_c , will still be determined by the liquid-crystal component of the binary system.

- [1] P.-G. De Gennes and J. Prost, *The Physics of Liquid Crystals*, International Series of Monographs on Physics Vol. 83 (Oxford University Press, New York, 1993).
- [2] C. Zannoni, *Liquid Crystals and their Computer Simulations* (Cambridge University Press, Cambridge, 2022).
- [3] I. Mušević and M. Škarabot, Self-assembly of nematic colloids, *Soft Matter* **4**, 195 (2008).
- [4] L. M. Lopatina and J. V. Selinger, Theory of ferroelectric nanoparticles in nematic liquid crystals, *Phys. Rev. Lett.* **102**, 197802 (2009).
- [5] L. Mesarec, S. Kralj, V. Kralj-Iglič, and A. Iglič, Complex soft matter configurations hosting nanoparticles and topological defects, in *Advances in Biomembranes and Lipid Self-Assembly*, edited by A. Iglič, M. Rappolt, and P. Losada-Pérez (Elsevier, New York, 2024), Vol. 39, pp. 41–56.
- [6] S. Orlandi, E. Benini, I. Miglioli, D. R. Evans, V. Reshetnyak, and C. Zannoni, Doping liquid crystals with nanoparticles. A computer simulation of the effects of nanoparticle shape, *Phys. Chem. Chem. Phys.* **18**, 2428 (2016).
- [7] G. Tiberio, L. Muccioli, R. Berardi, and C. Zannoni, Towards *in silico* liquid crystals. Realistic transition temperatures and physical properties for *n*-cyanobiphenyls via molecular dynamics simulations, *ChemPhysChem* **10**, 125 (2009).
- [8] E. Ouskova, O. Buchnev, V. Reshetnyak, Y. Reznikov, and H. Kresse, Dielectric relaxation spectroscopy of a nematic liquid crystal doped with ferroelectric $\text{Sn}_2\text{P}_2\text{S}_6$ nanoparticles, *Liq. Cryst.* **30**, 1235 (2003).
- [9] M. Čopič, A. Mertelj, O. Buchnev, and Y. Reznikov, Coupled director and polarization fluctuations in suspensions of ferroelectric nanoparticles in nematic liquid crystals, *Phys. Rev. E* **76**, 011702 (2007).
- [10] F. Li, O. Buchnev, C. I. Cheon, A. Glushchenko, V. Reshetnyak, Y. Reznikov, T. J. Sluckin, and J. L. West, Orientational coupling amplification in ferroelectric nematic colloids, *Phys. Rev. Lett.* **97**, 147801 (2006).
- [11] S. Kalashnikov, N. Romanov, and A. Nomoëv, Study of the properties of liquid crystals modified by nanoparticles, *J. Appl. Phys.* **119**, 094304 (2016).

- [12] F. G. Segura-Fernández, E. F. Serrato-García, J. E. Flores-Calderón, and O. Guzmán, Dynamics of nanoparticle self-assembly by liquid crystal sorting in two dimensions, *Front. Phys.* **9**, 636288 (2021).
- [13] C.-H. Chen and I. Dierking, Nanoparticles in thermotropic and lyotropic liquid crystals, *Front. Soft Matter* **4**, 1518796 (2025).
- [14] S. Starzonek, S. J. Rzoska, A. Drozd-Rzoska, K. Czupryński, and S. Kralj, Impact of ferroelectric and superparaelectric nanoparticles on phase transitions and dynamics in nematic liquid crystals, *Phys. Rev. E* **96**, 022705 (2017).
- [15] S. J. Rzoska, S. Starzonek, and A. Drozd-Rzoska, Pretransitional behavior and dynamics in liquid crystal-based nanocolloids, in *Advances in Colloid Science*, edited by M. M. Rahman and A. M. Asiri (IntechOpen, UK, 2016), pp. 450–469.
- [16] S. J. Rzoska, S. Starzonek, A. Drozd-Rzoska, K. Czupryński, K. Chmiel, G. Gaura, A. Michulec, B. Szczypek, and W. Walas, Impact of BaTiO₃ nanoparticles on pretransitional effects in liquid crystalline dodecylcyanobiphenyl, *Phys. Rev. E* **93**, 020701(R) (2016).
- [17] K. Górny, V. Raczyńska, P. Raczyński, Z. Dendzik, and S. Starzonek, Impact of polarized nanotube surface on ultrathin mesogen film properties: Computer simulation study, *Phys. Rev. E* **99**, 022701 (2019).
- [18] V. Raczyńska, K. Górny, P. Raczyński, Z. Dendzik, and S. Starzonek, Two-dimensional phases of confined 5-cyanobiphenyl: Computer simulation study, *Phys. Rev. E* **108**, 034702 (2023).
- [19] K. Górny, P. Raczyński, Z. Dendzik, and Z. Gburski, Odd-even effects in the dynamics of liquid crystalline thin films on the surface of single walled carbon and silicon carbide nanotubes: Computer simulation study, *J. Phys. Chem. C* **119**, 19266 (2015).
- [20] W. Gwizdała, V. Raczyńska, P. Raczyński, K. Górny, and Z. Dendzik, On the ordering of *n*-cyanobiphenyl mesogene molecules on graphene—a computer simulation study, *TASK Quarterly* **22**, 105 (2018).
- [21] D. Črešnar, C. Kyrou, I. Lelidis, A. Drozd-Rzoska, S. Starzonek, S. J. Rzoska, Z. Kutnjak, and S. Kralj, Impact of weak nanoparticle induced disorder on nematic ordering, *Crystals* **9**, 171 (2019).
- [22] J. Łoś, A. Drozd-Rzoska, S. J. Rzoska, S. Starzonek, and K. Czupryński, The fluctuation-driven dielectric properties of liquid crystalline 8OCB and its nanocolloids, *Soft Matter* **18**, 4502 (2022).
- [23] S. J. Rzoska, S. Starzonek, J. Łoś, A. Drozd-Rzoska, and S. Kralj, Dynamics and pretransitional effects in C₆₀ fullerene nanoparticles and liquid crystalline dodecylcyanobiphenyl (12CB) hybrid system, *Nanomaterials* **10**, 2343 (2020).
- [24] C. N. Mahyaoui, C. E. Goldmann, E. Garre, S. Mariot, I. Dozov, C. Meyer, and P. Davidson, Nanoparticles confined in liquid crystalline coatings with smectic focal-conic textures: Implications for precise nanoparticle positioning, *ACS Appl. Nano Mater.* **8**, 5207 (2025).
- [25] P. K. Mukherjee, Impact of ferroelectric nanoparticles on the dielectric constant of nematic liquid crystals, *Soft Mater.* **19**, 113 (2021).
- [26] Y. Garbovskiy and A. Glushchenko, Ferroelectric nanoparticles in liquid crystals: Recent progress and current challenges, *Nanomaterials* **7**, 361 (2017).
- [27] C. N. Melton, S. T. Riahinasab, A. Keshavarz, B. J. Stokes, and L. S. Hirst, Phase transition-driven nanoparticle assembly in liquid crystal droplets, *Nanomaterials* **8**, 146 (2018).
- [28] A. Humpert, S. F. Brown, and M. P. Allen, Molecular simulations of entangled defect structures around nanoparticles in nematic liquid crystals, *Liq. Cryst.* **45**, 59 (2018).
- [29] M. Urbanski, J. Mirzaei, T. Hegmann, and H.-S. Kitzerow, Nanoparticle doping in nematic liquid crystals: Distinction between surface and bulk effects by numerical simulations, *ChemPhysChem* **15**, 1395 (2014).
- [30] J. M. Ilnytskyi, A. Trokhymchuk, and M. Schoen, Topological defects around a spherical nanoparticle in nematic liquid crystal: Coarse-grained molecular dynamics simulations, *J. Chem. Phys.* **141**, 114903 (2014).
- [31] F. R. Hung and S. Bale, Faceted nanoparticles in a nematic liquid crystal: Defect structures and potentials of mean force, *Mol. Simul.* **35**, 822 (2009).
- [32] R. Richert, *Nonlinear Dielectric Spectroscopy* (Springer, New York, 2018).
- [33] F. Kremer and A. Schönhals, *Broadband Dielectric Spectroscopy* (Springer Science & Business Media, Berlin, 2002).
- [34] P. Biscari, G. Napoli, and S. Turzi, Bulk and surface biaxiality in nematic liquid crystals, *Phys. Rev. E* **74**, 031708 (2006).
- [35] G. R. Luckhurst and T. J. Sluckin, *Biaxial Nematic Liquid Crystals: Theory, Simulation and Experiment* (Wiley, New York, 2015).
- [36] K. Binder and A. P. Young, Spin glasses: Experimental facts, theoretical concepts, and open questions, *Rev. Mod. Phys.* **58**, 801 (1986).
- [37] P. M. Chaikin, T. C. Lubensky, and T. A. Witten, *Principles of Condensed Matter Physics* (Cambridge University Press, Cambridge, 1995), Vol. 10.
- [38] S. Kralj, Z. Bradač, and V. Popa-Nita, The influence of nanoparticles on the phase and structural ordering for nematic liquid crystals, *J. Phys.: Condens. Matter* **20**, 244112 (2008).
- [39] Y. Imry and S.-k. Ma, Random-field instability of the ordered state of continuous symmetry, *Phys. Rev. Lett.* **35**, 1399 (1975).
- [40] G. W. Gray, V. Vill, H. W. Spiess, D. Demus, and J. W. Goodby, *Physical Properties of Liquid Crystals* (Wiley, New York, 2009).
- [41] R. K. Iler, *The Chemistry of Silica: Solubility, Polymerization, Colloid and Surface Properties, and Biochemistry* (Wiley, New York, 1979), p. 866.
- [42] T. W. Stinson and J. Litster, Pretransitional phenomena in the isotropic phase of a nematic liquid crystal, *Phys. Rev. Lett.* **25**, 503 (1970).
- [43] I. Haller, Thermodynamic and static properties of liquid crystals, *Prog. Solid State Chem.* **10**, 103 (1975).
- [44] D. Liang, Liquid crystals in random environments, Ph.D. thesis, Johns Hopkins University, 2007.
- [45] A. Maritan, M. Cieplak, and J. R. Banavar, Nematic-isotropic transition in porous media, in *Liquid Crystals in Complex Geometries*, edited by G. P. Crawford and S. Zumer (CRC, Boca Raton, FL, 1996), pp. 483–496.
- [46] G. S. Iannacchione, G. P. Crawford, S. Žumer, J. W. Doane, and D. Finotello, Randomly constrained orientational order in porous glass, *Phys. Rev. Lett.* **71**, 2595 (1993).
- [47] P. J. Wojtowicz, P. Sheng, and E. Priestley, *Introduction to Liquid Crystals* (Springer, New York, 1975).

- [48] A. Majumdar and A. Zarnescu, Landau–De Gennes theory of nematic liquid crystals: the Oseen–Frank limit and beyond, *Arch. Ration. Mech. Anal.* **196**, 227 (2010).
- [49] O. M. Roscioni, L. Muccioli, R. G. Della Valle, A. Pizzirusso, M. Ricci, and C. Zannoni, Predicting the anchoring of liquid crystals at a solid surface: 5-cyanobiphenyl on cristobalite and glassy silica surfaces of increasing roughness, *Langmuir* **29**, 8950 (2013).
- [50] B. Jerome, Surface effects and anchoring in liquid crystals, *Rep. Prog. Phys.* **54**, 391 (1991).
- [51] L. Mirantsev, E. de Oliveira, I. de Oliveira, and M. Lyra, Defect structures in nematic liquid crystal shells of different shapes, *Liq. Cryst. Rev.* **4**, 35 (2016).